Original Article
Regulating TKT activity inhibits proliferation of human acute lymphoblastic leukemia cells

Fang-Liang Huang[1,2,3,4], Yao-Ming Chang[5], Cheng-Yung Lin[3], Sheng-Jie Yu[6,7,8], Jing-Tong Fu[9], Ting-Yu Chou[6], Sih-Wen Yeh[1], En-Chih Liao[3,10], Chia-Ling Li[1]

[1]Children's Medical Center, Taichung Veterans General Hospital, Taichung 407, Taiwan; [2]Department of Post-Baccalaureate Medicine, College of Medicine, National Chung Hsing University, Taichung 402, Taiwan; [3]Institute of Biomedical Sciences, MacKay Medical College, New Taipei 252, Taiwan; [4]Department of Physical Therapy, Hungkuang University, Taichung 433, Taiwan; [5]Institute of Biomedical Sciences, Academia Sinica, Taipei 115, Taiwan; [6]Department of Medical Research, Taichung Veterans General Hospital, Taichung 407, Taiwan; [7]Institute of Biomedical Sciences, College of Life Sciences, National Chung Hsing University, Taichung 402, Taiwan; [8]Integrated Care Center of Psoriatic Disease, Taichung Veterans General Hospital, Taichung 407, Taiwan; [9]Department of Pathology and Laboratory Medicine, Taichung Veterans General Hospital, Taichung 407, Taiwan; [10]Department of Medicine, MacKay Medical College, New Taipei 252, Taiwan

Abstract: Among pediatric blood cancers, acute lymphoblastic leukemia (ALL) is the most common hematologic malignancy. Within ALL, T-cell acute lymphoblastic leukemia (T-ALL) accounts for 10 to 15% of all pediatric cases, and ~25% of adult cases. For T-ALL, its recurrence and relapse after treatment remain problematic. Therefore, it is necessary to develop new therapies for T-ALL. Recent studies suggested regulating energy metabolism is a novel approach to inhibit tumor growth, likely a promising treatment. Transketolase (TKT) is an important enzyme for modulating glucose metabolize in the pentose phosphate pathway (PPP). In this study, we treated T-ALL cells with different doses of niclosamide and primary T-ALL PBMCs were analyzed by RNA sequencing. T-ALL cells treated with niclosamide were analyzed with the Western blotting and TKT activity assay. Metabolism of T-ALL cells was evaluated by ATP assay and seahorse analyses. Lastly, we used a T-ALL xenograft murine model to determine effects of TKT knockdown on T-ALL tumor growth. Tumor samples were analyzed by H&E and IHC stainings. We found that niclosamide reduced T-ALL cell viability, and reduced expressions of TKT, Transketolase-Like Protein 1/2 (TKTL1/2) and transaldolase. In addition, niclosamide inhibited TKT enzyme activity, aerobic metabolism and glycolysis, finally leading to lower production of ATP. TKT knockdown inhibited tumor growth of xenograft T-ALL mice. Findings showed that niclosamide inhibits T-ALL cell growth by inhibiting TKT and energy metabolism.

Keywords: T-cell acute lymphoblastic leukemia, transketolase, pentose phosphate pathway, energy metabolism, niclosamide

Introduction

T-cell acute lymphoblastic leukemia (T-ALL) is a hematologic malignancy characterized by the infiltration of immature T cell marker-expressing cells into the bone marrow. Accounting for 10 to 15% of pediatric ALL cases in Europe, the United States, and Japan, and 20 to 25% of adult ALL cases, T-ALL poses significant challenges in both pediatric and adult populations [1-3]. While pediatric T-ALL has notable advancements with an 85% overall complete remission rate, adult T-ALL lags behind with only a 40% remission rate, and a subset of patients remain refractory to standard chemotherapy [4, 5]. The recurrence of T-ALL, particularly in cases refractory to standard treatments, presents a pressing medical challenge. The high risk of relapse after the initial remission, coupled with the complexities of treatment upon recurrence, underscores the need for innovative therapeutic approaches [6]. One potential avenue lies in understanding the altered glucose metabolism characteristic of cancer cells, with a preference for glycolysis over oxidative phosphorylation, known as the

"Warburg effect". This type of metabolism facilitates rapid ATP production but results in the accumulation of metabolites [7, 8]. Targeting these metabolic pathways becomes a promising strategy for its treatment, given their pivotal role in sustaining cancer cell proliferation and immune evasion [9].

Transketolase (TKT), encoded by the TKT gene, emerges as a key player in connecting the pentose phosphate pathway (PPP) to glycolysis. Its overexpression has been implicated in various cancers, such as hepatocellular carcinoma, peritoneal metastases of ovarian cancer, and esophageal cancer, in promoting tumorigenesis through diverse mechanisms [10-12]. Advances in medical technology have unveiled the potential of targeting key enzymes like TKT in glycolysis to curb cancer progression [13]. However, the specific impact of TKT inhibition on T-ALL remains unexplored.

This study was aimed to bridge this knowledge gap by investigating the potential anticancer effects of targeting TKT in a T-ALL model. Our hypothesis was that TKT knockdown confers therapeutic benefits in treating T-ALL. The primary aim of this research was to provide valuable insights into innovative strategies for addressing the challenges associated with T-ALL and to broaden the repertoire of targeted therapeutic approaches for this hematologic malignancy.

Materials and methods

Cells and drug treatments

We maintained two human T-ALL cell lines: Jurkat and CCRF-CEM (obtained from the American Type Culture Collection; ATCC) at 37°C, in RPMI-1640 medium (Gibco; Thermo Fisher Scientific, Inc.) supplemented with the following: 10% heat-inactivated fetal bovine serum (FBS; HyClone; GE Healthcare Life Sciences), 1 mM sodium pyruvate (HyClone; GE Healthcare Life Sciences), 100 U/ml penicillin, and 100 μg/ml streptomycin (Invitrogen; Thermo Fisher Scientific, Inc.). Cells were kept in a humidified atmosphere containing 95% air and 5% CO_2. Cells were then treated with niclosamide (ACROS Organics™) at different doses and time courses.

Primary T-ALL cells

Primary T-ALL cells were harvested from PBMCs of either patient with T-ALL or healthy controls at the Taichung Veterans General Hospital. For PBMC culture, 8 mL of blood were collected in sodium citrate tubes (Vacutainer® CPT™, BD, USA) after being taken from patients or healthy controls. PBMCs were purified through centrifugation at a density gradient. Cells were cultured in RPMI-1640, supplemented with 10% fetal bovine serum, 1% penicillin/streptomycin, 25 mM HEPES, and 2 mM L-glutamine. The study protocol was approved by the Institutional Review Board of Taichung Veterans General Hospital, Taiwan (NO. CG19384A).

Isolation of RNA

Cells were collected from *in vitro* conditions, and harvested after drug treatments. Total RNA was extracted using the Amersham RNAspin Mini Kit (Cytiva) according to manufacturer's instructions.

RNA sequencing

The quality of the raw reads was checked using the FastQC (v0.11.9). Adapters, low quality bases and reads were trimmed with Trimmomatic (v0.36), using these parameters of ILLUMINACLIP: Adapter.fa:2:30:10 LEADING: 3 TRAILING: 3 SLIDINGWINDOW: 4:15 MINLEN: 36. After trimming, clean reads were aligned to the reference genome using HISAT2 (v2.2.1). StringTie (2.2.1) was used to normalize read counts. FeatureCounts (v1.6.2) were used to summarize reads. Differential expression analyses were performed using either DEGseq (v2.2.1) without biological replicates, or DESeq2 (1.34.0) with biological replicates. Differential expressions of gene sets were filtered based on the absolute value of $\log_2$ fold changes ≥2 with an adjusted *p*-value of <0.005 according to results of DEGseq. Differentially expressed gene sets at statistical significant levels were filtered based on the absolute value of $\log_2$ fold changes ≥2 and an adjusted *p*-value of <0.05 according to the results of DESeq2. To identify biological processes and pathways that are significantly enriched by the differentially expressed genes, the gene set enrichment analysis (i.e., GSEA) was performed

with the ClusterProfiler (4.2.2). The database of the Kyoto encyclopedia of genes and genomes (or KEGG) was used for annotation. Pathway visualization was performed using Pathview (1.34.0).

CCK-8 assay

Jurkat and CCRF-CEM cells were seeded at a density of $1×10^5$ cells/well in a 96-well cell culture plate. Jurkat and CCRF-CEM cells were treated at 37°C for 24 h, with either vehicle control (DMSO), α-Ketoglutarate (α-KG) or with niclosamide at different doses. Afterward, cell viability was determined with the CCK-8 kit (cat. no.96992, Sigma-Aldrich) according to the manufacturer's instructions. In addition, optical density was measured at 450 nm with a microplate reader (Enspire 2300-0000/Perkin-Elmer).

Western blot analysis

Jurkat and CCRF-CEM cells were seeded at a density of $1.5×10^6$ cells/well in a 12-well cell culture plate. Jurkat cells were treated with either vehicle control (DMSO) or niclosamide (1.0, 2.0 or 4.0 µM). CCRF-CEM cells were treated with either vehicle control (DMSO) or niclosamide (1.0, 2.0 or 4.0 µM). Both cell cultures were kept at 37°C for 24 h. After niclosamide treatments, cells were harvested and levels of protein expressions were determined using Western blotting with antibodies as appropriate. In brief, cells were first washed with PBS before collection. Cells were lysed in RIPA buffer (Biomed, Taiwan), and centrifuged at 13,000 g for 10 min at 4°C. Supernatant was used for protein quantification with a Coomassie protein assay reagent (Thermo Fisher Scientific, Inc.). Fixed amounts of protein (15 µg/lane) were loaded into each well and separated by SDS-PAGE. Samples were finally transferred to the PVDF membrane. Immunoblotting was conducted using the following antibodies: Transketolase (TKT) (cat. no. sc-390179; Santa Cruz; 1:1,000 dilution), Transketolase Like 1/2 (TKTL1/2) (cat. no. sc-514513; Santa Cruz; 1:500 dilution), Transaldolase (cat. no. sc-166230; Santa Cruz; 1:1,000 dilution) and β-actin (cat. no. 4970S; Cell Signaling Technology; 1:5,000 dilution), followed by incubation with secondary anti-mouse IgG, HRP-linked antibody (cat. no. 7076P2; Cell

Signaling Technology; 1:7,000 dilution) or goat anti-rabbit IgG antibody (cat. no. 7074P2; Cell Signaling Technology; 1:7,000 dilution). Labeled proteins were detected using the ECL Detection Kit (Millipore) obtained from Alliance Q9 (UVITEC, UK). Normalization was performed with the β-actin antibody.

Measuring ATP levels

ATP measurements were carried out with the ATP Assay Kit Colorimetric/Fluorometric kit (ab83355, Abcam, USA) according to the manufacturer's instructions. In brief, $1×10^6$ cells were washed in cold PBS and then homogenized in 100 µl of ATP assay buffer. Cells were centrifuged at 4°C at 13,000 g, before the supernatant was collected. Standard samples were prepared according to the manufacturer's instructions. Test samples and background controls were prepared in a 96-well plate according to the manufacturer's instructions for colorimetric assay. Finally, plates were read on a plate reader (Enspire 2300-0000/PerkinElmer) at OD 570 nm.

TKT activity assay

TKT activity was measured with the Transketolase Activity Assay Kit (Fluorometric) (ab-273310, Abcam, USA) according to the manufacturer's instructions. In brief, cells $(4×10^5)$ were homogenized in a 100 µl TKT Assay buffer for lysis, and then centrifuged at 4°C at 10,000 g. Supernatants were then collected. Standard samples were prepared according to the manufacturer's instructions. Test samples and background control were prepared in a 96-well plate according to the manufacturer's instructions for fluorometric assay. Fluorescence was measured immediately at 30 sec intervals for 30 to 45 min at 37°C with a plate reader (Enspire 2300-0000/PerkinElmer).

Seahorse analyses

Cells were plated in Seahorse XF 6-well plates at respective optimal densities one day prior to measurements. Cells were placed in experimental conditions as described above, and incubated in Seahorse XF Assay Media at 37°C for 1 hr without CO_2 just before assay. Substrate concentrations were as follows: 1 µM for Oligo and FCCP, 1 µM/0.5 µM for Rot/AA, and 5 mM for succinate. All reagents were

obtained from Seahorse Bioscience. Basic conditions of glycolysis, maximal glycolytic capacity, and non-glycolytic activity were measured with the Seahorse XF-6 Extracellular Flux Analyzer.

T-ALL xenograft murine model

Female NOD/SCID mice aged 8 weeks with body weight between 18 and 22 g were obtained from the National Laboratory Animal Center (Taipei, Taiwan). Mice were housed under specific pathogen-free conditions with 12:12-h dark/light cycle, with *ad libitum* food and water supply. All experiments were approved by the Animal Care and Use Committee of Kaohsiung Veterans General Hospital (IACUC NO. 2021-2022-A003-MOST) and the Animal Care and Use Committee of Taichung Veterans General Hospital (IACUC NO. La-1111910). CCRF-CEM cells (1×10^6 cells/100 µl/mouse), suspended in a 1:1 mixture of BD Matrigel^{TM} (basement membrane matrix, growth factor reduced, phenol red-free; BD Biosciences, cat. no. 356231) and RPMI-1640 medium were injected subcutaneously into the flank region of each NOD/SCID mouse. Tumors were periodically measured with a digital caliper 3 times/week until sacrifice. Mice were randomly divided into different experiment groups (6 mice/group) as follows: (a) vehicle control group, (b) niclosamide (20 mg/kg) treatment group, (c) α-KG (10 mg/kg) treatment group, and (d) α-KG (10 mg/kg) plus niclosamide (20 mg/kg) treatment group. Niclosamide and α-KG were delivered through intraperitoneal injections, 3 times/week, beginning on day 7 after induction. Mice were sacrificed on day 28, with tumor samples collected for H&E and IHC stainings.

Hematoxylin and eosin (H&E) staining

Tumor tissues were removed from the xenograft mice and fixed in 10% formalin for 24 h at room temperature. Tissues were embedded in paraffin, and then sectioned for staining with hematoxylin and eosin (H&E). Microscopic images were captured through a light microscope (AXIOVERT, ZEISS).

Immunohistochemistry (IHC) staining

After tumor tissues had been removed from the xenograft mice, specimens were fixed in 10% phosphatebuffered formalin, dissected and then embedded in paraffin. Paraffin sections (3 µm in thickness) were incubated with 0.3% hydrogen peroxide for 15 min, blocked for 1 h at room temperature, and then incubated with Transketolase (TKT) (cat. no. sc-390179; Santa Cruz) and Ki-67 (cat. no. 9449S; Cell Signaling Technology) overnight at 4°C. After washing with TBST, sections were processed with the Epredia^{TM} UltraVision^{TM} Quanto Detection System HRP DAB kit (Epredia^{TM} TL-060-QHD), and whenever required, stained with DAB immediately (Epredia^{TM}).

Statistical analyses

Data were expressed as mean ± standard error of mean. Statistical analyses were performed using oneway ANOVA followed by Tukey's test for *post-hoc* comparisons. Results were analyzed using the software GraphPad Prism (version 6; GraphPad Software, Inc.). Statistical significance was set at $P < 0.05$.
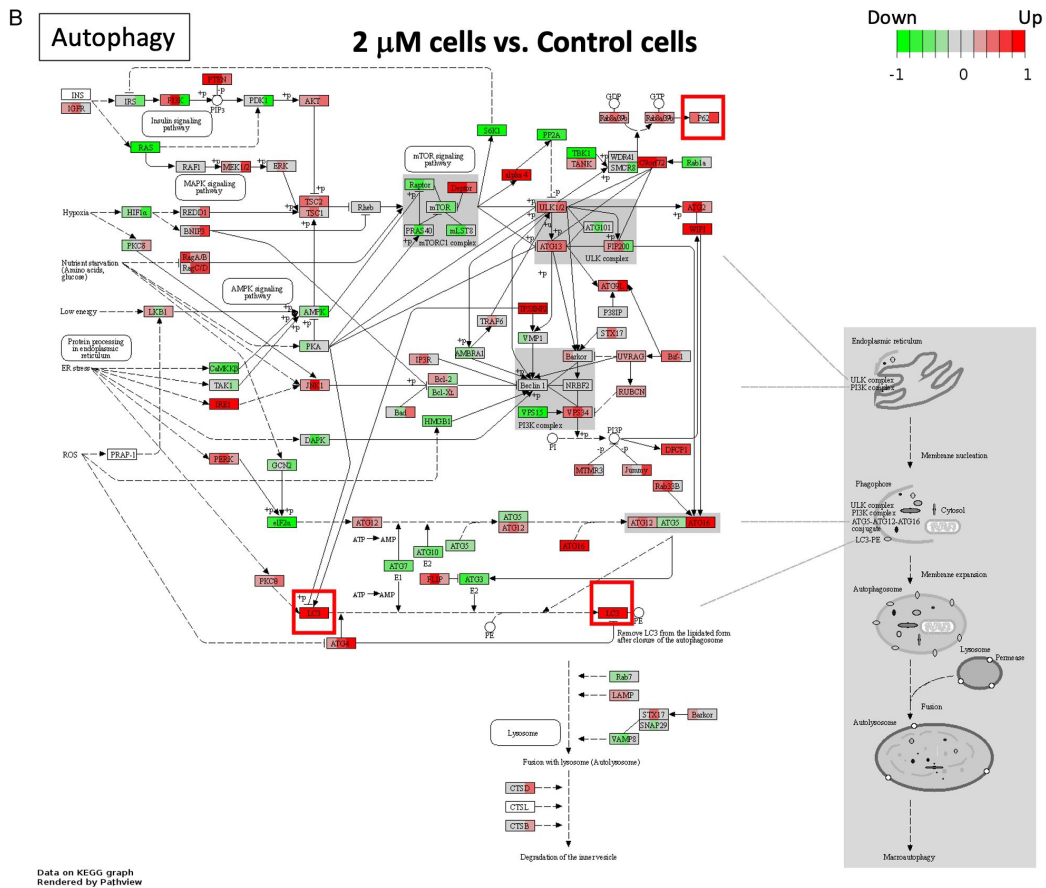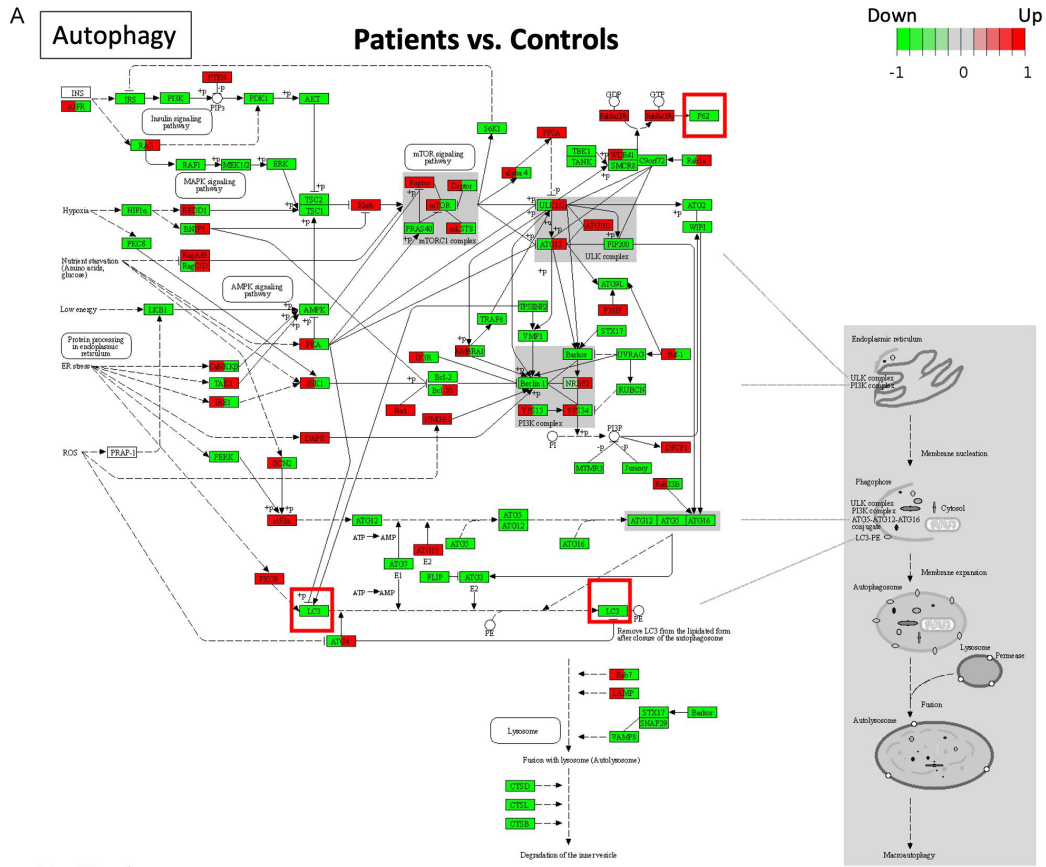
Results

Down-regulation of autophagy in T-ALL

We have previously reported that niclosamide suppresses tumor growth of T-cell acute lymphoblastic leukemia through the activation of apoptosis and autophagy [14]. Here, we further compared expressions of autophagy-related genes between clinical PBMC samples obtained from T-ALL patients and healthy controls. KEGG autophagy pathway graph rendered by Pathview revealed down-regulated genes (in green), such as LC3 and p62 (**Figure 1A**) that are involved in the autophagic pathway in T-ALL patients' PBMC samples when compared with healthy controls. On the other hand, the same genes showed significant up-regulations in niclosamide-treated CCRF-CEM cells when compared with WT CCRF-CEM cells (**Figure 1B**).

*Suppression of TKT remarkably diminishes T-ALL cell viability*

To investigate the impact of TKT downregulation on the viability of T-ALL cells, we subjected CCRF-CEM and Jurkat cells to 24 hrs treatment with niclosamide or a well-established TKT inhibitor, α-KG. Results showed a dose-dependent reduction in T-ALL cell viability induced by

TKT modulation as a therapeutic strategy for T-ALL

A

Patients vs. Controls

B

2 μM cells vs. Control cells

Figure 1. KEGG pathway graph rendered by Pathview. KEGG Pathview showing autophagy pathway genes up or down regulated in (A) T-ALL patients vs. healthy control and in (B) niclosamide (2 mM; 24 h) treated CCRF-CEM cells compared to WT CCRF-CEM cells.
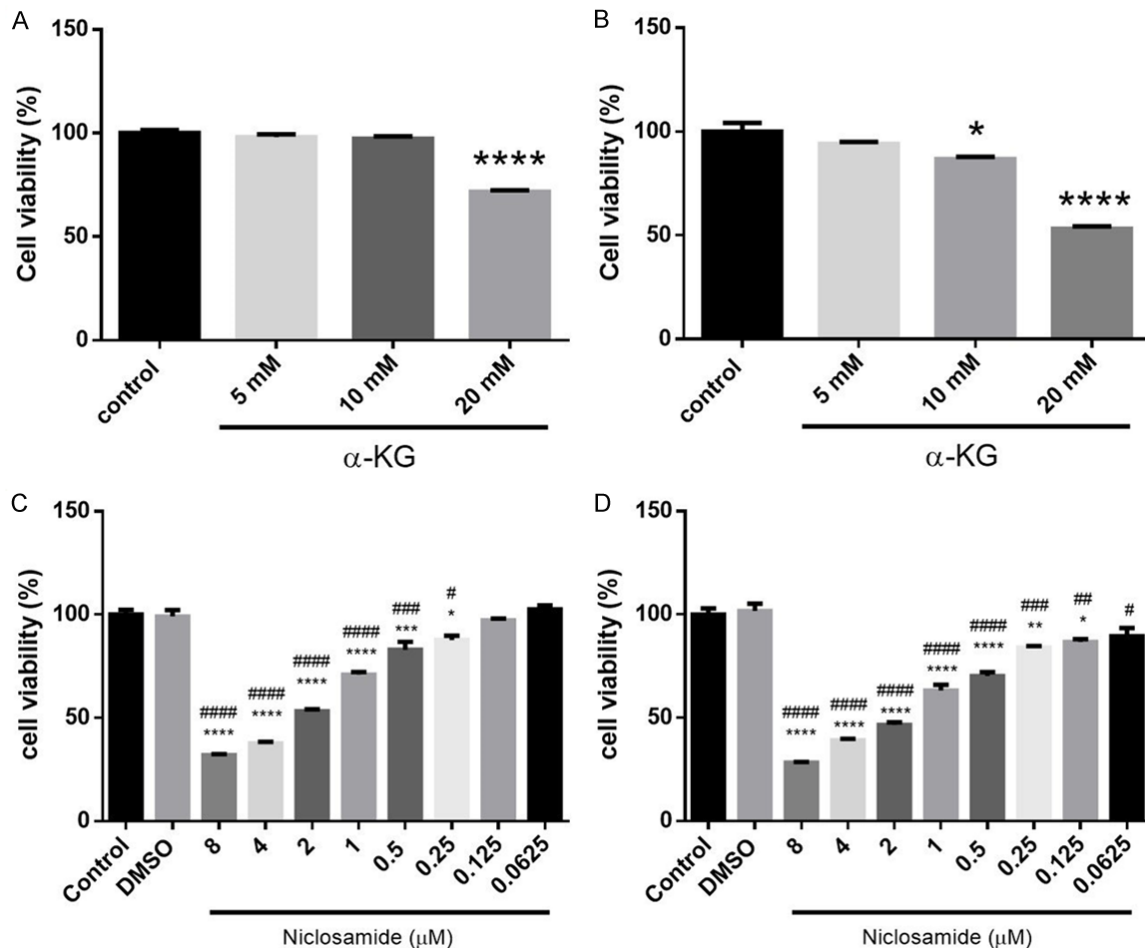
Figure 2. α-KG and niclosamide effectively inhibits the viability of T-ALL cells in a dose-dependent manner. Human T-ALL cells were treated with α-KG or niclosamide for 24 h. Cell viability and proliferation was measured by CCK-8 assays. CCK-8 assays showed that α-KG and niclosamide inhibited the proliferation of (A, C) CCRF-CEM and (B, D) Jurkat cells dose-dependently. The results are expressed as mean ± SEM. *$P<0.05$, **$P<0.01$, ***$P<0.001$, ****$P<0.0001$, vs. the control group; #$P<0.05$, ##$P<0.01$, ###$P<0.001$, ####$P<0.0001$, vs. the DMSO group.

α-KG and niclosamide (**Figure 2**). This underscores the critical role of TKT in sustaining T-ALL cell viability, suggesting the potential significance of targeted interventions against TKT for therapeutic purposes.

TKT downregulation impairs ATP production in T-ALL cells

As illustrated in **Figure 2**, the observed cancer cell deaths may be intricately linked to a reduction in energy metabolism resources. Therefore, we further explore potential shifts in the final ATP production after TKT downregula-

tion. CCRF-CEM and Jurkat cells were initially subjected to different doses of α-KG or niclosamide, in addition to a vehicle control, over a 24-hour period. Results showed a decline in ATP production in α-KG- or niclosamide-treated CCRF-CEM and Jurkat cells, when compared with vehicle controls (**Figure 3**). Moreover, both α-KG and niclosamide exhibited a significant, dose-dependent inhibition of ATP production. Taken together, these findings robustly suggest that both α-KG and niclosamide exert a dose-dependent inhibition on ATP production in T-ALL cells. This finding supports the pivotal involvement of TKT
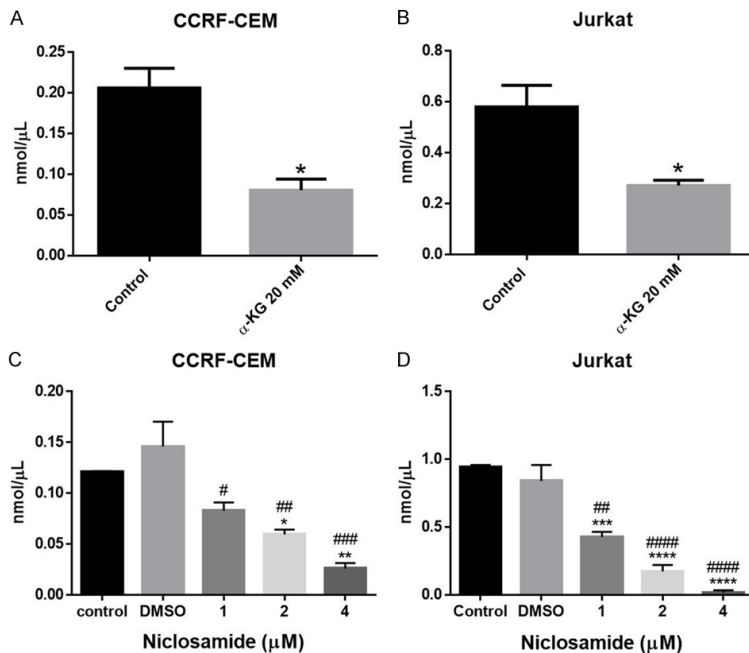
Figure 3. α-KG and niclosamide effectively inhibits ATP production of T-ALL cells dose-dependently. The cells were treated with different doses of α-KG or niclosamide for 24 h. ATP production were measured by ATP assays. *$P<0.05$, **$P<0.01$, ***$P<0.001$, ****$P<0.0001$, vs. the control group; #$P<0.05$, ##$P<0.01$, ###$P<0.001$, ####$P<0.0001$, vs. the DMSO group. DMSO group: vehicle control group.

in finely regulating cellular energy homeostasis. Such insights underscore the potential therapeutic efficacy of targeting TKT to perturb ATP production, thereby impeding the survival mechanisms of T-ALL cells.

Niclosamide targets key protein expressions in the pentose phosphate pathway of T-ALL cells

Metabolic reprogramming is considered a hallmark of cancer development. To generate energy, cancer cells prefer glycolysis over oxidative phosphorylation. Most leukemias are highly dependent on glycolysis and can be targeted using glycolytic inhibitors. TKT, TKTL1/2 and transaldolase (TALDO1) play important roles in connecting the pentose phosphate pathway (PPP) to glycolysis. Therefore, to investigate niclosamide effects on protein expressions related to the PPP, CCRF-CEM and Jurkat human T leukemia cells were initially treated with different doses of niclosamide or vehicle control for 24 h. Results showed that niclosamide had inhibited expressions of PPP pathway-related proteins, such as TKT, TKTL1/2 and transaldolase, in CCRF-CEM and Jurkat cells in a dose-dependent manner (**Figure 4A**, **4B**). Taken

together, niclosamide had inhibited PPP related protein expressions of T-ALL cells in a dose-dependent manner.

Downregulation of TKT inhibits TKT activity in T-ALL cells

TKT, a key enzyme in the non-oxidative phase of PPP, crucially links glycolysis with PPP. As shown in **Figure 4**, niclosamide treatment reduced TKT protein levels, prompting an exploration into potential changes in TKT enzyme activity. To further investigate this issue, CCRF-CEM and Jurkat cells underwent a 24-hour treatment with α-KG, niclosamide, or a vehicle control. Notably, both α-KG and niclosamide (at 4 μM) effectively inhibited TKT activity within the initial 45 minutes in both cell lines (**Figure 5**). Findings suggested a significant suppression of TKT activity in T-ALL cells following treatment with α-KG and niclosamide.

Niclosamide inhibits mitochondrial aerobic metabolism and glycolysis in T-ALL cells

Furthermore, we used the Seahorse machine to measure oxygen consumption rate (OCR) and extracellular acidification rate (ECAR) in T-ALL cells. We evaluated glycolysis by analyzing the ECAR, and also measured the mitochondrial aerobic metabolism based on OCR. We found that both OCR and ECAR were inhibited after niclosamide treatment (**Figures 6**, **7**). In response to niclosamide, we observed significant inhibitions in ATP-production coupled respiration (**Figure 6**) and glycolysis (**Figure 7**). Findings suggested that niclosamide treatment, through the inhibition of TKT, had effectively suppressed mitochondrial aerobic metabolism and glycolysis in T-ALL cells.

Improving xenograft T-ALL mouse model phenotype through TKT downregulation

To validate the findings of *in vitro* experiments, where inhibition of TKT impeded T-ALL cell growth, we further applied a known TKT inhibi-
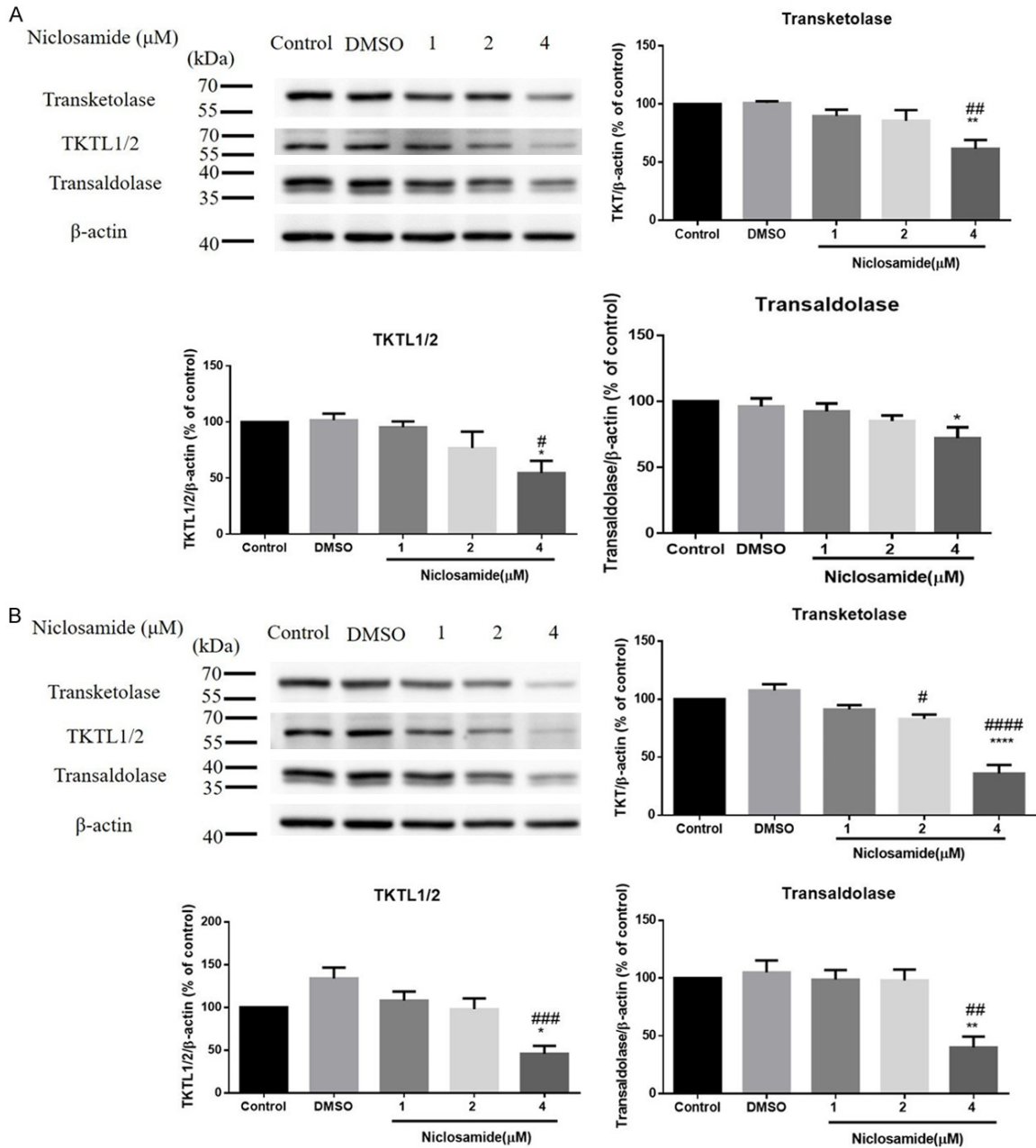
Figure 4. Niclosamide inhibits TKT, TKTL1/2 and transaldolase expressions of T-ALL cells in a dose-dependent manner. The cells were treated with different doses of niclosamide for 24 h, and the expression of TKT, TKTL1/2 and transaldolase were measured by western blot analysis in (A) CCRF-CEM and (B) Jurkat cells. β-actin protein was used in these experiments as the loading control. The results are expressed as mean ± SEM. *P<0.05, **P<0.01, ****P<0.0001, vs. the control group; #P<0.05, ##P<0.01, ###P<0.001, vs. the DMSO group. DMSO group: vehicle control group.

tor, α-KG, to treat the xenograft T-ALL mice. The primary objective was to determine whether the inhibition of TKT also results in suppressing tumor growth *in vivo*. In brief, to confirm that the metabolic alterations induced by TKT downregulation can impact cancer growth *in vivo*,

we conducted experiments using the xenograft T-ALL murine model. Results showed a substantial reduction in tumor volume upon TKT downregulation through α-KG administration (**Figure 8**). Notably, both niclosamide treatment and combined niclosamide plus α-KG treat-
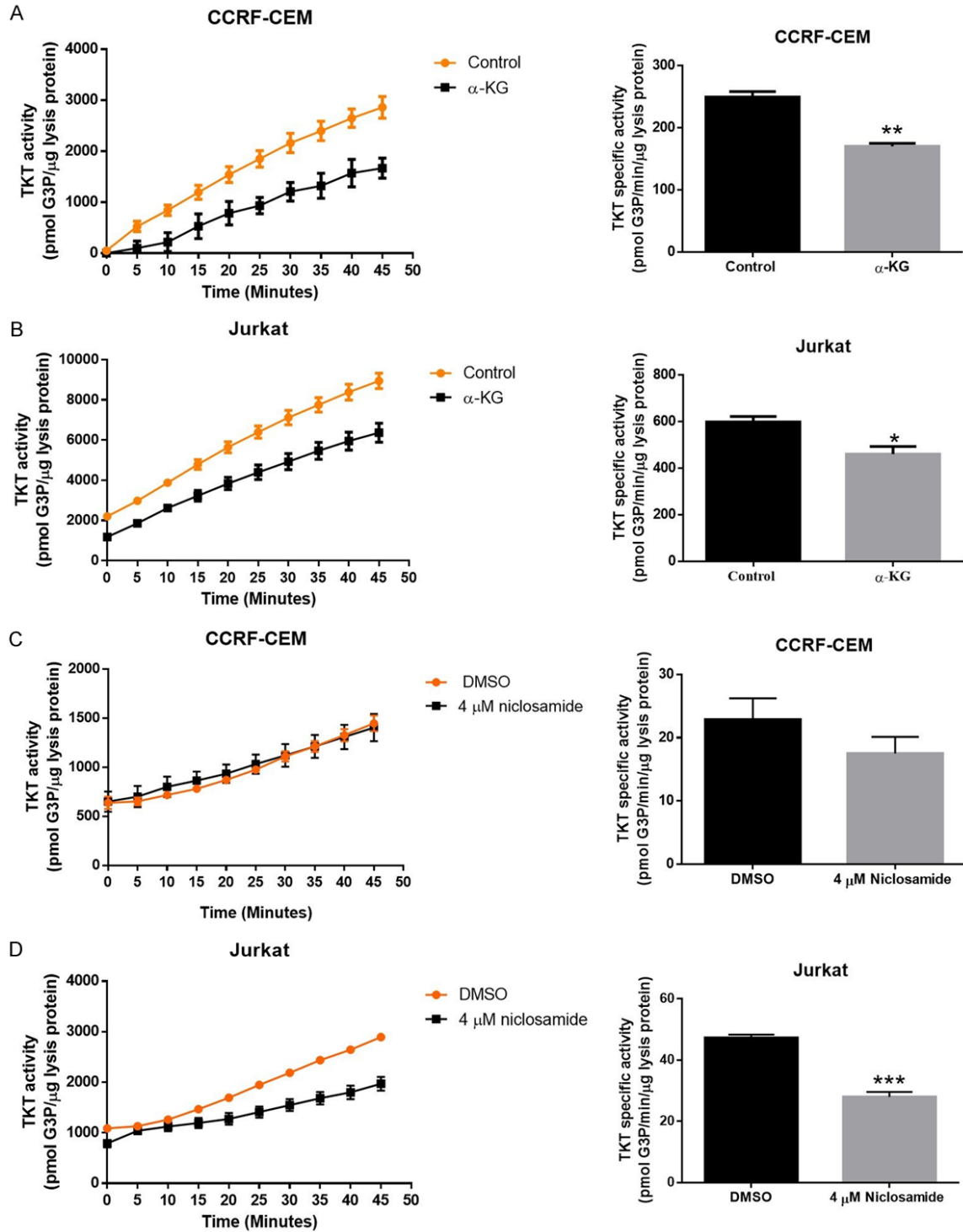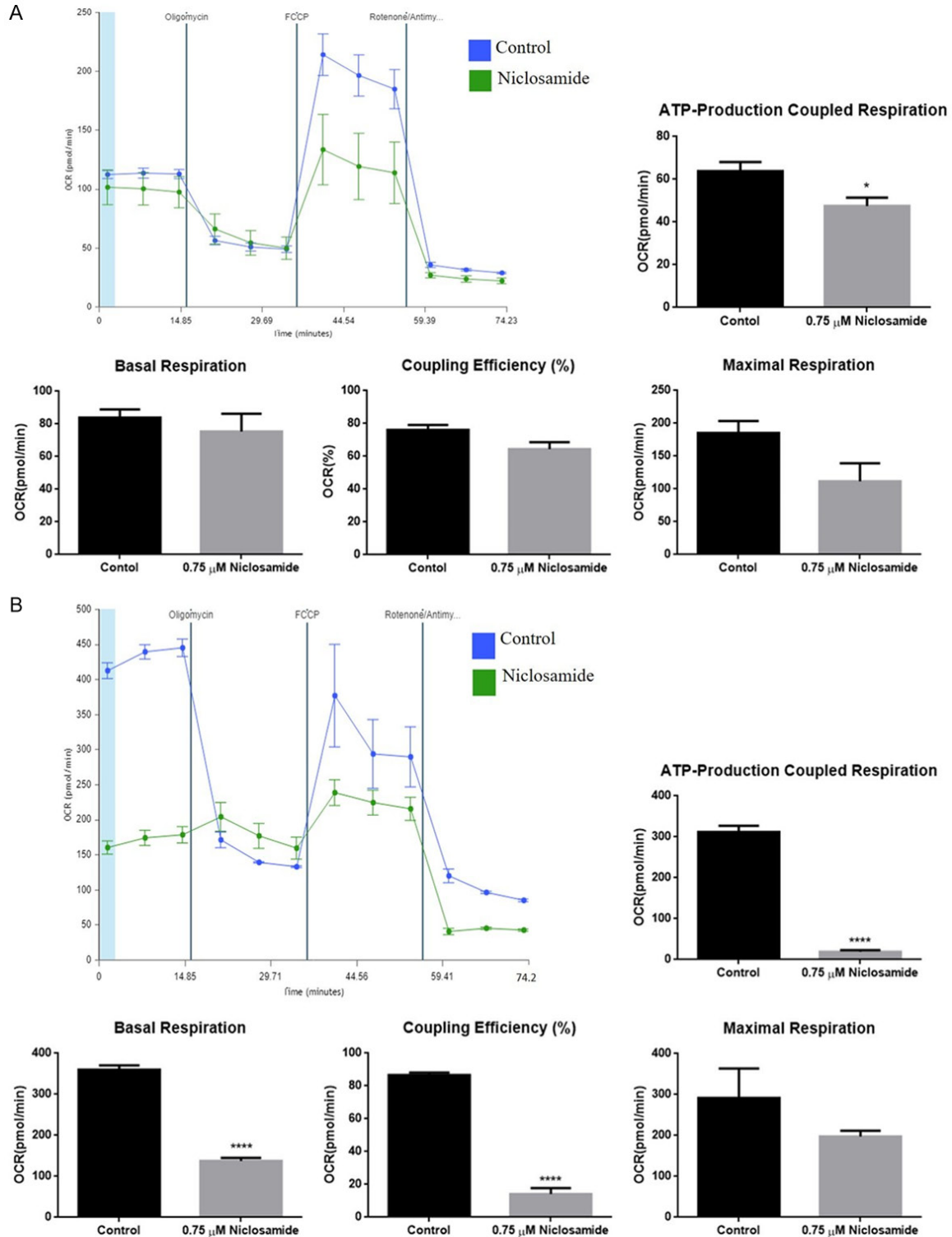
Figure 5. α-KG and niclosamide treatment inhibits TKT activity in T-ALL cells. The cells were treated with α-KG (20 mM) or niclosamide (4 μM) for 24 h. The absolute specific TKT activities were determined and then compared. The results are expressed as mean ± SEM. *P<0.05, **P<0.01, ***P<0.001.

ment also produced significant reductions in tumor volume compared with vehicle controls, underscoring the pivotal role of targeting TKT in inhibiting T-ALL tumor growth.

Figure 6. Niclosamide treatment affects mitochondrial oxygen consumption in T-ALL cells. Niclosamide treatment decreased oxygen consumption rate (OCR) in (A) CCRF-CEM and (B) Jurkat cells. Following a sequential addition of inhibitors of mitochondrial function: oligomycin, carbonyl cyanide-p trifluoromethoxyphenylhydrazone (FCCP), and a combination of rotenone and antimycin A. Maximal respiration was measured following the addition of FCCP. The results are expressed as mean ± SEM. *P<0.05, ****P<0.0001 vs. control group.

A

B
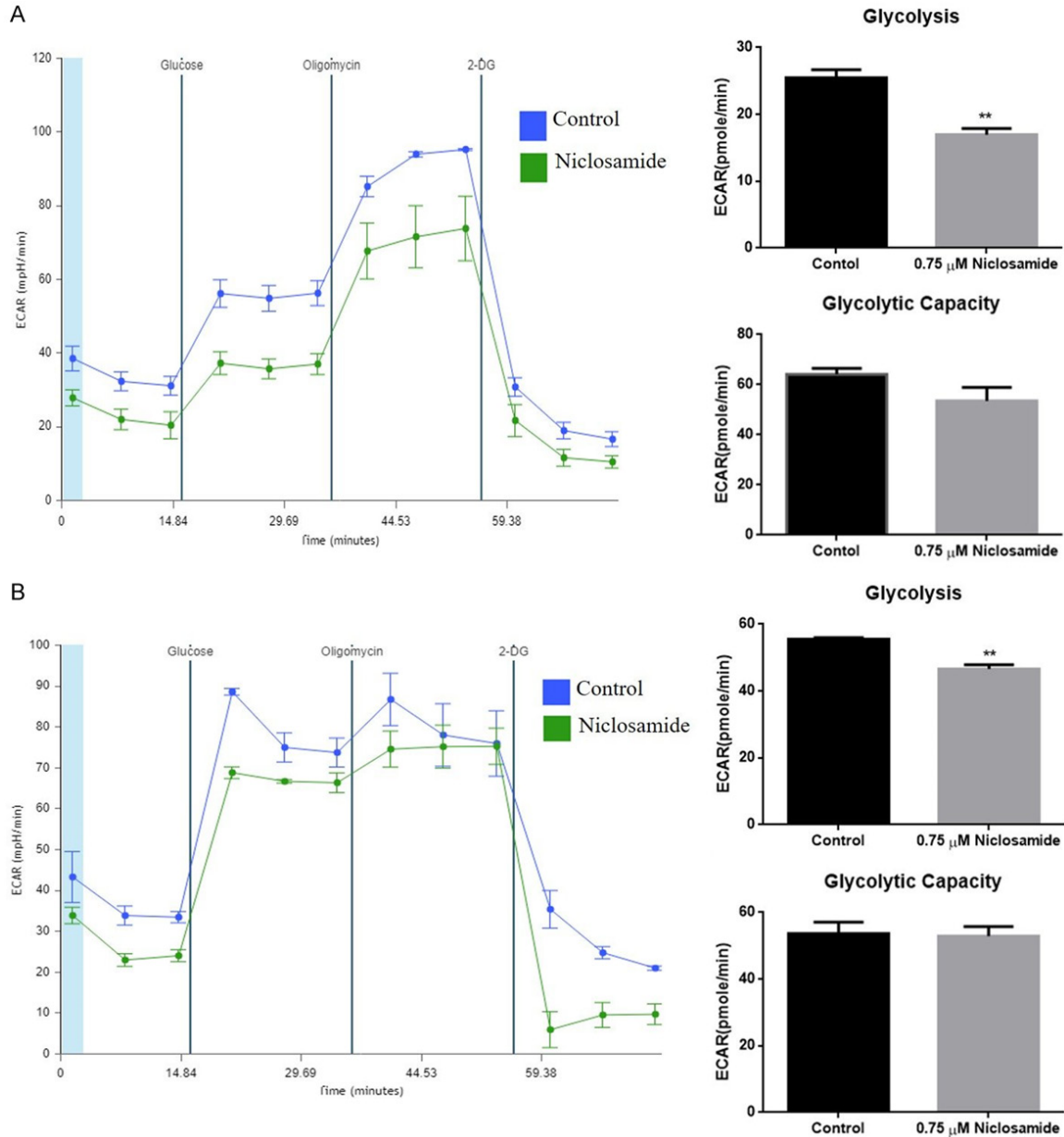
Figure 7. Niclosamide treatment affects extracellular acidification rate (ECAR) in T-ALL cells. Niclosamide treatment decreased extracellular acidification rate (ECAR), non-glycolytic acidification and glycolytic capacity in (A) CCRF-CEM and (B) Jurkat cells. The results are expressed as mean ± SEM. **$P < 0.01$, vs. control group.

Niclosamide improves pathology of xenograft T-ALL mice

Since downregulation of TKT inhibited tumor growth in xenograft T-ALL mice, we further investigated whether downregulation of TKT improves the pathology of xenograft T-ALL mice. Tumor samples were therefore examined using the H&E and IHC stainings. H&E staining showed that tumor masses contained leuke-mia cells, with a discohesive pattern of medium to large atypical lymphoid cells displaying signs of brisk apoptosis and mitotic activity. Compared with the vehicle controls, the experimental groups showed more degenerative tumor cells with smudge nuclei and more cell apoptosis associated with niclosamide treatment, α-KG treatment and α-KG plus niclosamide treatments (**Figure 9A**). IHC staining showed that TKT and Ki-67 expressions were
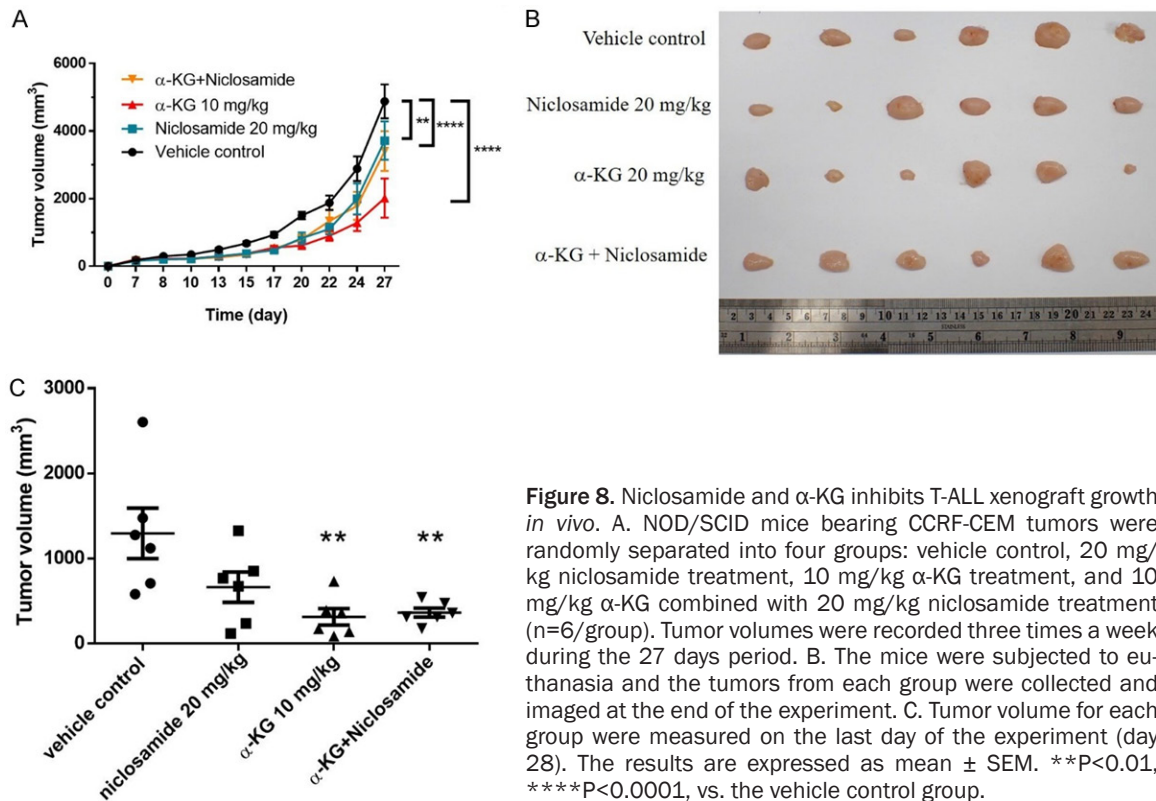
Figure 8. Niclosamide and α-KG inhibits T-ALL xenograft growth *in vivo*. A. NOD/SCID mice bearing CCRF-CEM tumors were randomly separated into four groups: vehicle control, 20 mg/kg niclosamide treatment, 10 mg/kg α-KG treatment, and 10 mg/kg α-KG combined with 20 mg/kg niclosamide treatment (n=6/group). Tumor volumes were recorded three times a week during the 27 days period. B. The mice were subjected to euthanasia and the tumors from each group were collected and imaged at the end of the experiment. C. Tumor volume for each group were measured on the last day of the experiment (day 28). The results are expressed as mean ± SEM. **P<0.01, ****P<0.0001, vs. the vehicle control group.

both lowered with niclosamide, α-KG and α-KG plus niclosamide treatments compared with the vehicle controls (**Figure 9B**, **9C**).

Downregulation of PPP-related genes by niclosamide

Further bioinformatics analysis of CCRF-CEM cells treated with niclosamide revealed downregulation of key enzymes related to PPP. They included TKT, transaldolase and G6PD (**Figure 10A**). The enrichment plot and heat map of differentially expressed genes indicated marked suppressions of PPP in niclosamide-treated CCRF-CEM cells. Gene Set Enrichment Analysis (GSEA) revealed that the PPP genes were highly enriched in control CCRF-CEM cells, with a concomitant drop in expressions of TKT, transaldolase and G6PD in niclosamide-treated CCRF-CEM cells (**Figure 10B**). Taken together, niclosamide was found to inhibit key enzymes of PPP in T-ALL cells.

Discussion

Our study underscored a pivotal role for niclosamide in inhibiting T-ALL cell viability by targeting the glycolysis pathway and its associated proteins, including TKT activity. The inhibition of ATP production, involving both mitochondrial aerobic metabolism and glycolysis, suggested a broader impact on the energy metabolism crucial for the survival of T-ALL cells. Importantly, downregulation of TKT was found to impede tumor growth in a xenograft T-ALL mouse model, affirming that TKT is a significant player in T-ALL progression.

Metabolic reprogramming is a hallmark of cancer, characterized by increased glucose consumption to support abnormal cell growth and survival in the challenging tumor microenvironment [15]. TKT, a major reversible enzyme in the nonoxidative branch of the pentose phosphate pathway (PPP) [16], is upregulated in various tumors, like colorectal cancer [17], ovarian cancer [11] and lung adenocarcinoma [18]. However, its expression in T-ALL has remained unknown. Our study revealed, in T-ALL, the suppressed expressions of PPP-related proteins, including TKT, TKTL1/2, and transaldolase, further establishing TKT as a prognostic biomarker and therapeutic target.
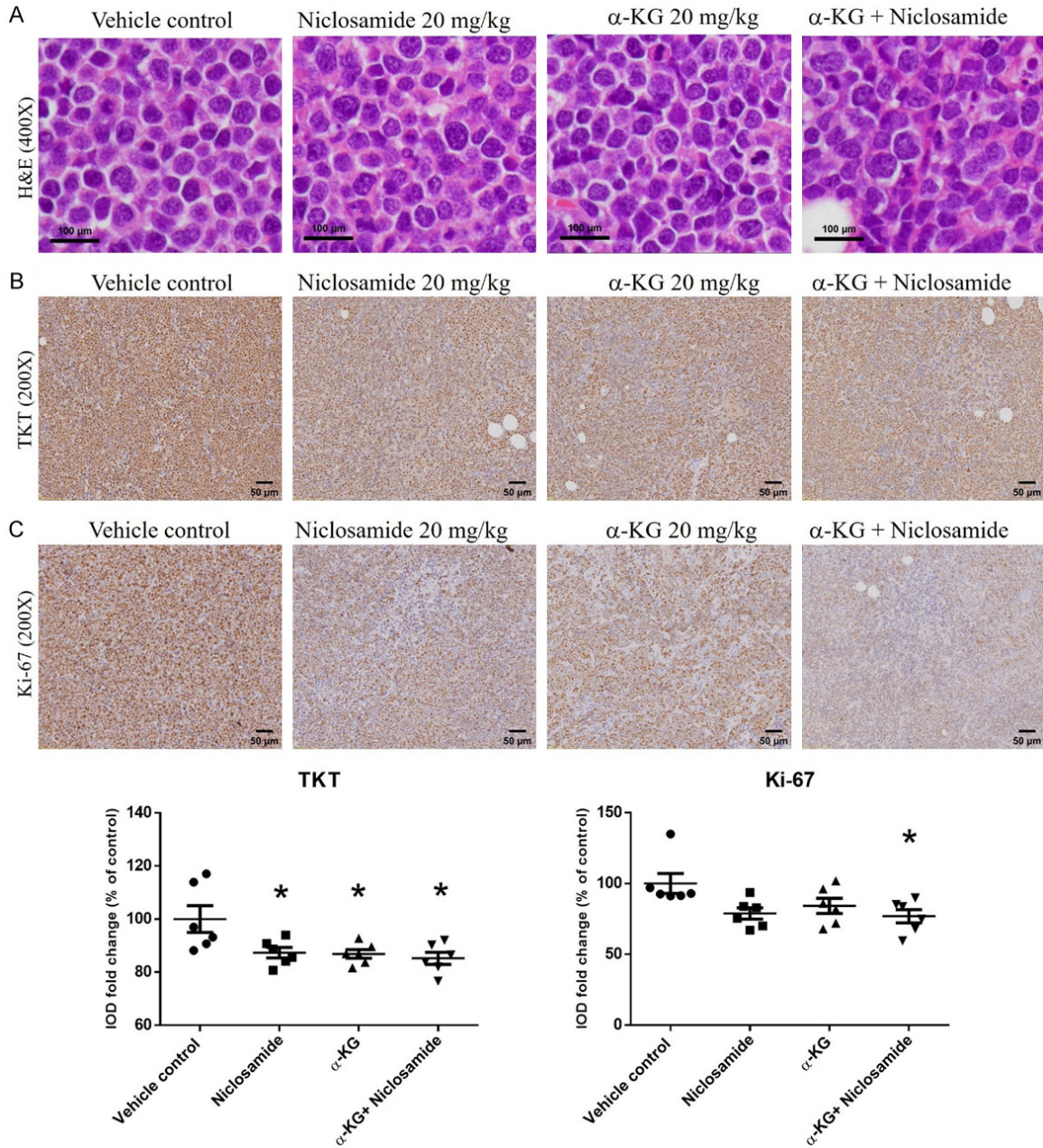
Figure 9. Niclosamide suppresses xenograft tumor proliferation and inhibits the production of TKT and Ki-67 in NOD/SCID mice. Tumor samples were subjected to (A) H&E staining and IHC analysis for (B) TKT and (C) Ki-67 at the end of the experiment. Slides were scanned on magnifications of ×400 and ×200. H&E, hematoxylin and eosin; IHC, immunohistochemistry. *P<0.05, vs. the vehicle control group.

In our study, we observed the suppressed expression of TKT in T-ALL, aligning with the notion of altered metabolism in cancer cells. This downregulation of TKT significantly impeded T-ALL cell viability and tumor growth, highlighting its functional importance in T-ALL progression. Our findings contribute to the growing body of evidence in support of the potential therapeutic relevance of targeting TKT in cancer treatment. The broader context of cancer metabolism further accentuates the significance of TKT as a therapeutic target. Cancer cells exhibit a preference for aerobic glycolysis, known as the Warburg effect, to meet their energy demands [19]. TKT's role in connecting glycolysis to the PPP positions it as a key medi-
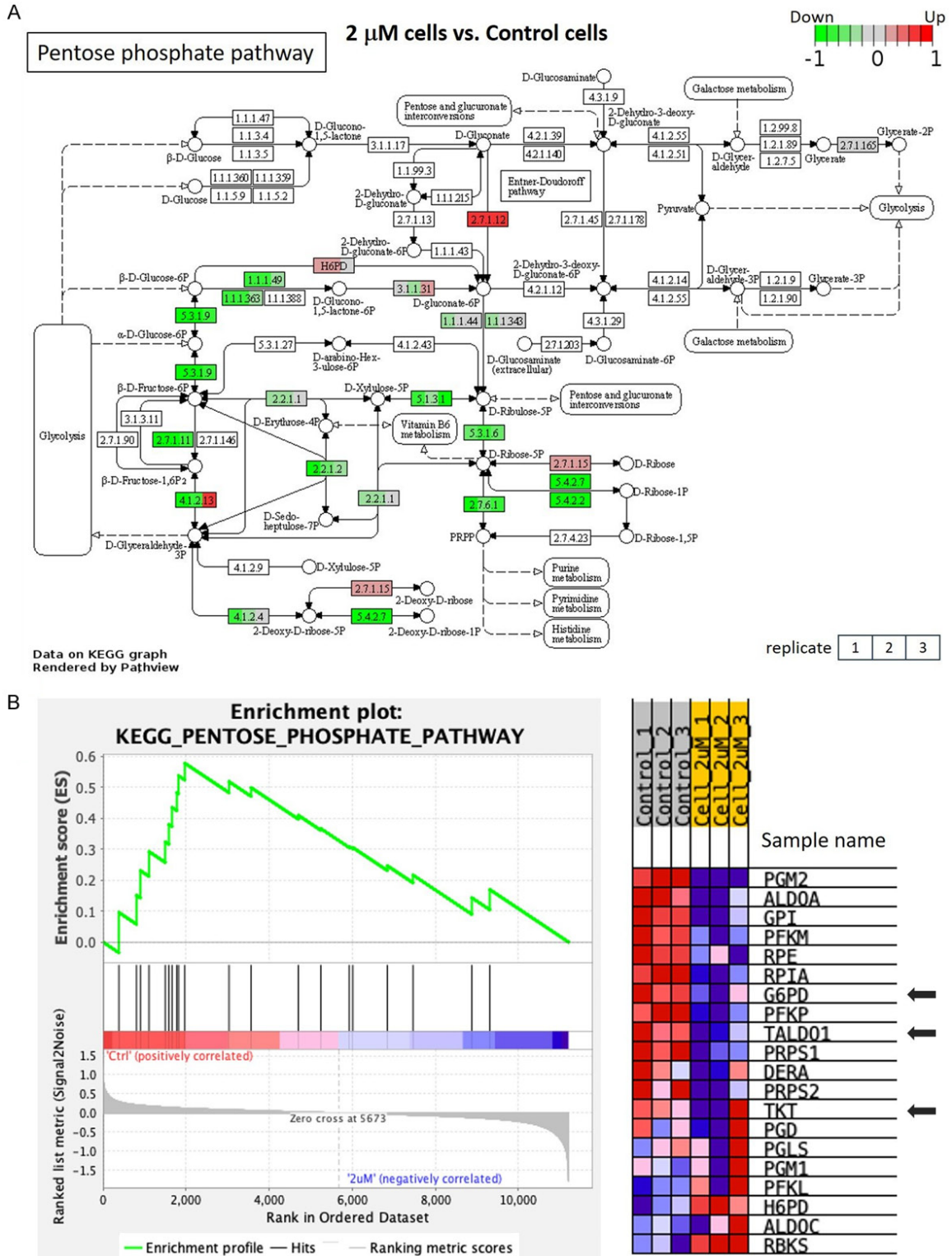
Figure 10. KEGG pathway graph rendered by Pathview and GSEA enrichment plots. KEGG Pathview showing pentose phosphate pathway genes up or down regulated in (A) niclosamide (2 mM; 24 h) treated CCRF-CEM cells compared to WT CCRF-CEM cells. In (A), enzyme 2.2.1.1: transketolase; enzyme 2.2.1.2: transaldolase; enzyme: 1.1.1.49: G6PD. (B) GSEA enrichment plots of the HALLMARK PENTOSE PHOSPHATE PATHWAY and the corresponding heat map for control versus niclosamide (2 mM) treatment groups in CCRF-CEM cells. Transaldolase: TALDO1; Transketolase: TKT. G6PD: Glucose 6 phosphate dehydrogenase.

ator of this metabolic shift. Targeting TKT not only impacts nucleotide synthesis but also disrupts the interconnected metabolic pathways essential for cancer cell survival and growth.

Maintaining stable glucose metabolism is an important requirement for the survival and progression of cancer cells. Cancer cells rely on aerobic glycolysis to meet metabolic demands. Cancer cell growths is dominated by metabolism switching from mitochondrial respiration to glycolysis during hypoxia [20, 21]. In our study, we found that niclosamide inhibited ATP production of T-ALL, and through inhibitions of aerobic metabolism and glycolysis, especially by suppressing expressions and activities of those enzymes in PPP, to reduce energy resources of cancer cells, leading to cell death. Our results are consistent with previous reports. Many compounds have anticancer effects in preclinical experiments. These compounds include Phloretin, WZB117, Fasentin are glucose transporter blockers [22, 23]. Another glucose analog, 2-deoxyglucose (2-DG), showed promising anticancer effects in preclinical models. This 2-DG glucose analog, which inhibits glycolysis and depletes ATP, has been used to treat lymphoma [24] and breast cancer [25]. Therefore, based on our previous findings and results from the literature, tumor glycolysis appears to be an ideal target for therapeutic intervention.

Numerous studies have highlighted niclosamide's anticancer effects, attributing them to apoptosis, inhibition of migration, invasion, and proliferation [26]. Our results further emphasize niclosamide as a potent TKT inhibitor, significantly reducing TKT activity and, consequently, suppressing T-ALL cell proliferation and tumor growth. Importantly, the observed inhibition of aerobic metabolism and glycolysis in cancer cells underscores niclosamide's efficacy in reducing their energy resources. While our findings support the anti-leukemia effect of niclosamide through downregulating TKT and altering energy metabolism, our experiments combining α-KG with niclosamide did not yield a superior effect *in vivo*. The absence of synergistic effects observed when combining α-KG with niclosamide can be attributed to several factors. Firstly, if the drugs share similar mechanisms of action, their effects may compete

rather than enhance each other. This phenomenon is well-discussed in the context of cancer signaling pathways [27]. Secondly, optimal therapeutic concentrations and doses may differ for each drug, making it challenging to achieve a synergistic outcome [28]. Finally, the intricate cellular network and feedback mechanisms within a biological system may interact in a complex manner, contributing to the lack of observed synergy [29]. These factors highlight the need for careful consideration and optimization when designing drug combinations, consistent with the multifaceted nature of drug-drug interactions in therapeutic contexts. This discrepancy warrants careful consideration in future studies.

Acknowledging the limitations of our study, including a small clinical sample size and the potential for enhanced understanding through the establishment of a TKT knockout mice model, our results contribute to the growing body of evidence highlighting niclosamide's efficacy in targeting altered metabolism in T-ALL.

In conclusion, our study not only shedded light on the crucial role of altered metabolism in T-ALL but also explicitly connected this discussion to the rationale for targeting TKT. The inhibition of TKT by niclosamide emerges as a promising therapeutic strategy, influencing the broader context of cancer metabolism and providing a foundation for future investigations and clinical applications.

Disclosure of conflict of interest

None.

Address correspondence to: Dr. Chia-Ling Li, Children's Medical Center, Taichung Veterans General Hospital, 1650 Taiwan Boulevard Sect. 4, Taichung 407, Taiwan. E-mail: lingboxer@gmail.com; Dr. En-Chih Liao, Department of Medicine, Mackay Medical College, No. 46, Sec. 3, Zhongzheng Rd., Sanzhi Dist., New Taipei 252, Taiwan. E-mail: enchih@mmc.edu.tw

References

[1] Van Vlierberghe P and Ferrando A. The molecular basis of T cell acute lymphoblastic leukemia. J Clin Invest 2012; 122: 3398-3406.

[2] Peirs S, Van der Meulen J, Van de Walle I, Taghon T, Speleman F, Poppe B and Van Vlierberghe P. Epigenetics in T-cell acute lymphoblastic leukemia. Immunol Rev 2015; 263: 50-67.

[3] Tasian SK, Loh ML and Hunger SP. Childhood acute lymphoblastic leukemia: integrating genomics into therapy. Cancer 2015; 121: 3577-3590.

[4] Tanosaki R and Tobinai K. Adult T-cell leukemia-lymphoma: current treatment strategies and novel immunological approaches. Expert Rev Hematol 2010; 3: 743-753.

[5] Samra B, Jabbour E, Ravandi F, Kantarjian H and Short NJ. Evolving therapy of adult acute lymphoblastic leukemia: state-of-the-art treatment and future directions. J Hematol Oncol 2020; 13: 70.

[6] Huguet F and Tavitian S. Emerging biological therapies to treat acute lymphoblastic leukemia. Expert Opin Emerg Drugs 2017; 22: 107-121.

[7] Chae YC and Kim JH. Cancer stem cell metabolism: target for cancer therapy. BMB Rep 2018; 51: 319-326.

[8] Deshmukh A, Deshpande K, Arfuso F, Newsholme P and Dharmarajan A. Cancer stem cell metabolism: a potential target for cancer therapy. Mol Cancer 2016; 15: 69.

[9] Gill KS, Fernandes P, O'Donovan TR, McKenna SL, Doddakula KK, Power DG, Soden DM and Forde PF. Glycolysis inhibition as a cancer treatment and its role in an anti-tumour immune response. Biochim Biophys Acta 2016; 1866: 87-105.

[10] Qin Z, Xiang C, Zhong F, Liu Y, Dong Q, Li K, Shi W, Ding C, Qin L and He F. Transketolase (TKT) activity and nuclear localization promote hepatocellular carcinoma in a metabolic and a non-metabolic manner. J Exp Clin Cancer Res 2019; 38: 154.

[11] Ricciardelli C, Lokman NA, Cheruvu S, Tan IA, Ween MP, Pyragius CE, Ruszkiewicz A, Hoffmann P and Oehler MK. Transketolase is upregulated in metastatic peritoneal implants and promotes ovarian cancer cell proliferation. Clin Exp Metastasis 2015; 32: 441-455.

[12] Chao YK, Peng TL, Chuang WY, Yeh CJ, Li YL, Lu YC and Cheng AJ. Transketolase serves a poor prognosticator in esophageal cancer by promoting cell invasion via epithelial-mesenchymal transition. J Cancer 2016; 7: 1804-1811.

[13] Hu LH, Yang JH, Zhang DT, Zhang S, Wang L, Cai PC, Zheng JF and Huang JS. The TKTL1 gene influences total transketolase activity and cell proliferation in human colon cancer LoVo cells. Anticancer Drugs 2007; 18: 427-433.

[14] Huang FL, Yu SJ, Liao EC, Li LY, Shen PW and Li CL. Niclosamide suppresses T-cell acute lymphoblastic leukemia growth through activation of apoptosis and autophagy. Oncol Rep 2022; 47: 30.

[15] Faubert B, Solmonson A and DeBerardinis RJ. Metabolic reprogramming and cancer progression. Science 2020; 368: eaaw5473.

[16] Hao S, Meng Q, Sun H, Li Y, Li Y, Gu L, Liu B, Zhang Y, Zhou H, Xu Z and Wang Y. The role of transketolase in human cancer progression and therapy. Biomed Pharmacother 2022; 154: 113607.

[17] Li M, Zhao X, Yong H, Xu J, Qu P, Qiao S, Hou P, Li Z, Chu S, Zheng J and Bai J. Transketolase promotes colorectal cancer metastasis through regulating AKT phosphorylation. Cell Death Dis 2022; 13: 99.

[18] Niu C, Qiu W, Li X, Li H, Zhou J and Zhu H. Transketolase serves as a biomarker for poor prognosis in human lung adenocarcinoma. J Cancer 2022; 13: 2584-2593.

[19] Vander Heiden MG, Cantley LC and Thompson CB. Understanding the Warburg effect: the metabolic requirements of cell proliferation. Science 2009; 324: 1029-1033.

[20] Hu Y, Lu W, Chen G, Wang P, Chen Z, Zhou Y, Ogasawara M, Trachootham D, Feng L, Pelicano H, Chiao PJ, Keating MJ, Garcia-Manero G and Huang P. K-ras(G12V) transformation leads to mitochondrial dysfunction and a metabolic switch from oxidative phosphorylation to glycolysis. Cell Res 2012; 22: 399-412.

[21] Lu W, Hu Y, Chen G, Chen Z, Zhang H, Wang F, Feng L, Pelicano H, Wang H, Keating MJ, Liu J, McKeehan W, Wang H, Luo Y and Huang P. Novel role of NOX in supporting aerobic glycolysis in cancer cells with mitochondrial dysfunction and as a potential target for cancer therapy. PLoS Biol 2012; 10: e1001326.

[22] Liu Y, Cao Y, Zhang W, Bergmeier S, Qian Y, Akbar H, Colvin R, Ding J, Tong L, Wu S, Hines J

and Chen X. A small-molecule inhibitor of glucose transporter 1 downregulates glycolysis, induces cell-cycle arrest, and inhibits cancer cell growth in vitro and in vivo. Mol Cancer Ther 2012; 11: 1672-1682.

[23] Macheda ML, Rogers S and Best JD. Molecular and cellular regulation of glucose transporter (GLUT) proteins in cancer. J Cell Physiol 2005; 202: 654-662.

[24] Zagorodna O, Martin SM, Rutkowski DT, Kuwana T, Spitz DR and Knudson CM. 2-deoxyglucose-induced toxicity is regulated by Bcl-2 family members and is enhanced by antagonizing Bcl-2 in lymphoma cell lines. Oncogene 2012; 31: 2738-2749.

[25] Repas J, Zügner E, Gole B, Bizjak M, Potočnik U, Magnes C and Pavlin M. Metabolic profiling of attached and detached metformin and 2-deoxy-D-glucose treated breast cancer cells reveals adaptive changes in metabolome of detached cells. Sci Rep 2021; 11: 21354.

[26] Wang Z, Ren J, Du J, Wang H, Liu J and Wang G. Niclosamide as a promising therapeutic player in human cancer and other diseases. Int J Mol Sci 2022; 23: 16116.

[27] Yap TA, Omlin A and de Bono JS. Development of therapeutic combinations targeting major cancer signaling pathways. J Clin Oncol 2013; 31: 1592-1605.

[28] Le Tourneau C, Lee JJ and Siu LL. Dose escalation methods in phase I cancer clinical trials. J Natl Cancer Inst 2009; 101: 708-720.

[29] Kitano H. Cancer as a robust system: implications for anticancer therapy. Nat Rev Cancer 2004; 4: 227-235.